RSC Advances

This is an *Accepted Manuscript*, which has been through the Royal Society of Chemistry peer review process and has been accepted for publication.

Accepted Manuscripts are published online shortly after acceptance, before technical editing, formatting and proof reading. Using this free service, authors can make their results available to the community, in citable form, before we publish the edited article. This *Accepted Manuscript* will be replaced by the edited, formatted and paginated article as soon as this is available.

You can find more information about *Accepted Manuscripts* in the **Information for Authors**.

ROYAL SOCIETY OF CHEMISTRY

www.rsc.org/advances

A Novel Benzothiazole Derivative SKLB826 Inhibits Human Hepatocellular Carcinoma Growth *Via* Inducing G2/M Phase Arrest and Apoptosis

Qian Lei[a,c], Lidan Zhang[b,c], Yong Xia[a], Tinghong Ye[a], Fangfang Yang[a], Yongxia Zhu[a], Xuejiao Song[a], Ningyu Wang[a], Ying Xu[a], Xiaowei Liu[a], Luoting Yu[a,*]

[a] State Key Laboratory of Biotherapy and Cancer Center, West China Hospital, Sichuan University, and Collaborative Innovation Center for Biothrapy. Chengdu 610041, China, [b] Department of Pharmaceutical and Bioengineering, School of Chemical Engineering, Sichuan University, Chengdu 610041, China;

[c] These authors contributed equally to this work.

* Corresponding author, Tel: +86 28 85503817; fax: +86 28 85164060; E-mail address: yuluot@scu.edu.cn

RA-ART-03-2015-005387

Hepatocellular carcinoma is the fifth most common cancer and durable responses in conventional treatments are limited so that researchers have been devoted to develop new anti-HCC agents. Benzothiazole derivatives are known for various biological activities and received considerable attention in cancer therapy, hence we designed and synthesized a novel potent benzothiazole compound 2-chloro-N-(2-(2-(2-morpholino-2-oxoethyl)thio)-2,3-dihydrobenzo[d]thiazol-6-yl)aceta mide (SKLB826) and further investigated the biological activities against cancer. The results suggested that SKLB826 showed growth inhibition against a broad spectrum of human cancer cells, especially human HCC cell lines, in a dose-dependent manner and induced G2/M phase arrest *via* down-regulating the CDK1, cyclinA2 and cdc25c protein levels. SKLB826 could also induce apoptosis of HCC cells *via* decreasing the expression of Bcl-2 and increasing the levels of BAX and cleaved caspase3, 9. Moreover, after treatment with SKLB826, the change of ROS level and $\Delta\Psi m$ suggesting that SKLB826 might induce apoptosis through intrinsic mitochondrial apoptotic pathway. Furthermore, SKLB826 could suppress tumor growth in HepG2 xenograft model without inducing any notable major organ-related toxicity, suggesting that SKLB826 may be a potential candidate for HCC therapy.

Introduction

Hepatocellular carcinoma (HCC) has been the fifth most common cause of cancer and also the second most common cause of cancer-related mortality in the world which only ranks after lung cancer [1,2]. Conventional treatments like liver transplantation and chemotherapy are used to treat HCC but the therapeutic outcomes are far away from satisfactory because of poor responses, severe toxicities and high recurrence rates [3].

Therefore, there is still an urgent need to develop anti-HCC agents with better activity and less toxicity.

Cell cycle plays an important role in cancer cell proliferation, which is an essential mechanism for tumor growth [4]. Aberrant cell cycle regulation may induce the growth of tumors, providing a new direction for cancer therapy [5,6]. At present, many cytotoxic agents targeting the cell cycle *via* inducing the G0/G1 or G2/M phase arrest, such as PD-0332991 (PhaseⅢ) [7] and LEE-011 (Phase Ⅲ) [8], have been under clinical evaluation and have achieved exciting therapeutic effects. Moreover, cell cycle arrest can lead to apoptosis of tumor cells [9]. There are two kinds of apoptotic pathways, namely cell death receptor-mediated extrinsic pathway and mitochondria-mediated intrinsic pathway [10,11]. Most types of chemotherapeutic drugs induce apoptosis through intrinsic pathway [12]. It is mainly controlled by caspase family and Bcl-2 family members, showing another direction of cancer therapies [13]. Therefore, drugs that could inhibit cell cycle progression and induce apoptosis may be effective to treat human HCC.

Benzothiazole derivatives display diverse biological properties, including antidiabetic and antitumor activities [14], and attract researchers' interests for developing them into anticancer drugs. Our research group put many efforts into investigating the anticancer properties of the benzothiazole derivatives. A series of benzothiazole derivatives with different structures had been synthesized and screened for their anticancer efficacy, some of them exhibited excellent anticancer activities *in vitro* [15]. Among them ,
2-chloro-N-(2-(2-(5-chloropyridin-2-ylamino)-2-oxoethylthio)benzo[d]thiazol-6-yl) acetamide (SKLB826) showed strong anti-proliferation activities in various cancer cell lines in MTT assay. Interestingly, we found that human liver cancer cell lines were more sensitive to SKLB826 than other cancer cell lines. Therefore, we further investigated the anti-cancer effects and the mechanisms underlying the inhibition of HCC *in vitro* and *in vivo*. The results in our study showed that SKLB826 might be a promising novel anti-HCC drug candidate which is worth further investigation.

Meterials and methods

Compounds and reagents

2-chloro-N-(2-(2-(2-morpholino-2-oxoethyl)thio)-2,3-dihydrobenzo[d]thiazol-6-yl)acetamide (SKLB826) was obtained through design, synthesis and optimization on benzothiazole derivatives for anti-tumor activity. The synthetic route was shown in Fig.1. Briefly, the starting material 1 was prepared from morpholine and 2-chloroacetyl chloride. Treatment of 6-aminobenzo[*d*]thiazole-2-thiol with 1 in THF provided 2. This was followed by 2-chloroacetyl chloride treatment of a mixture of 2 and K_2CO_3 and SKLB826 was obtained. Its structure formula was shown in Fig.1B. The compound was dissolved in dimethyl sulfoxide (DMSO) at a stock concentration of 40 mM and diluted in the relevant medium in all *in vitro* experiments. SKLB826 was dissolved in ultrapure water and Cremophor EL/ethanol (50:50; Sigma Cremophor EL, 95% ethyl alcohol) for *in vivo* studies.

Materials

3-(4,5-Dimethylthiazol-2-yl)-2,5-diphenyltetrazolium bromide (MTT), dimethyl sulfoxide (DMSO), Rhodamine-123 (Rh123), propidium iodide (PI), Hoechst 33342 were purchased from Sigma (St.Louis, MO). The Annexin V-FITC apoptosis detection kit was purchased from KeyGEN Biology Co. Ltd (Nanjing, China). The antibodies against cleaved caspase-9, Bcl-2 and Bax were obtained from Cell Signaling Technology Company (Beverly, MA), and the other primary antibodies were purchased from Abcam (Cambridge, MA, USA). Antibody against β-actin was acquired from Santa Cruz Biotechnology Company (Santa Cruz, CA).

Cell culture

The human HCC cell lines Bel7402 and SMMC-7721 were obtained from the China Center for Type Culture Collection (CTCCC, Wuhan, China). All the other human cancer cell lines used in our study were obtained from the American Type Culture Collection (ATCC). The cells were maintained in DMEM or RPIM 1640 medium supplemented with 10% fetal bovine serum and 0.1% amikacin sulfate and incubated in a humidified atmosphere at 37℃ with 5% CO_2.

Cell viability Assay

The effects of SKLB826 on cell viability were assessed by using MTT assay. Briefly, a number of $2\text{-}5\times10^{3}$ cells/well in 100 μL were seeded in 96-well plates 24 h before the experiment and then 100 μL of medium with various concentrations of SKLB826 (40, 20, 10, 5, 2.5, 1.25, 0 μM) was added and incubated for 24, 48 and 72 h, respectively. Then 20 μL of MTT (5 mg/mL) was added to each well and incubated for an additional 2~4 h. The medium was removed and 150 μL DMSO was added to dissolve the formazan crystal. The absorbance of each well was measured using a Spectra Max M5 microplate spectrophotometer (Molecular Devices) at 570 nm wavelength. Then the percentage of inhibition and IC_{50} values were calculated. Each assay was repeated 3 times.

The colony formation assay

The cells (800 cells/well) were seeded in a 6-well plate 24 h before the experiment, then 2 mL of medium with indicated concentrations of SKLB826 was added to each well and incubated for another two weeks. The cells were stained by 0.5% crystal violet solution after washed with PBS and fixed with methanol. The colonies were counted to assess the rate of inhibition. Each assay was repeated 3 times.

Morphological analysis of nuclei of HCC cells

Cells were plated onto 18-mm cover glass in a 6-well plate 24 h before the experiment and treated with SKLB826 for 48 h. Then Hoechst33342 was added to the wells in the dark for 15 min. The stained cells were observed and taken photos under fluorescence microscope (zeiss, Axiovert 200, Germany).

Cell cycle and apoptosis analysis by Flow Cytometry (FCM)

Cell cycle was analyzed by PI assay. Briefly, harvested cells were stained with propidium iodide (PI) after washed twice with 2 mL of PBS and fixed with 75% ethanol. Then the stained cells were assayed by FCM (BD Biosciences). Data were analyzed *via* using Modfit 2.8 software.

We also detected the apoptosis induced by SKLB826 *via* using the Annexin V-FITC apoptosis detection kit. Cells were incubated with Annexin V-FITC and PI for 15 min in the dark, then the stained cells were detected by FCM and the data were analyzed with FlowJo software.

Mitochondrial membrane potential (ΔΨm) assay

Mitochondrial membrane potential of cancer cells were determined after staining with Rh123 and detecting by FCM as described previously [16,17]. Mitochondrial membrane potential was detected *via* using Rh123, HepG2 and Bel7402 cells were treated with indicated doses of SKLB826 for 24 h and then incubated with 5 μg/mL Rh123 for 30 min in the dark. Then cells were harvested and washed with cold PBS, fluorescence emitted from Rh123 was detected by FCM.

ROS levels assay

DCFH-DA was applied to detect the ROS levels of cancer cell lines. After treatment with SKLB826 for 24 h, HepG2 and Bel7402 cells were incubated with PBS containing 10 μM DCFH-DA for 30 min at 37 . Then cells were washed with cold PBS and the ROS levels were detected by FCM.

Western blotting analysis

Cancer cells were treated with SKLB826 for indicated time and lysed in RIPA buffer (added with PMSF) on ice for 30 min. Then the cell lysates were centrifuged at 13000 g at 4 for 20 min, the supernatant was harvested and the protein concentration was determined by the BCA method. Equal amounts of protein were resolved by SDS-PAGE and transferred onto polyvinylidene difluoride (PVDF) membranes (Amersham Bioscience, Piscataway, NJ). After incubation with the specific primary and secondary antibodies, the protein bands were visualized using an enhanced chemiluminescent substrate to horseradish peroxidase (Amersham, Piscataway, NJ)

Subcutaneous xenograft models

The animal experiments were approved and conducted in accordance with the Animal Care and Use Committee of Sichuan University. To investigate the antitumor activity of SKLB826 *in vivo*, 100 μL tumor cell suspension containing 1×10^7 cells were injected subcutaneously into the right-flanks of female BALB/c nude mice (6 weeks old). When average volume of the tumors reached to about 150 mm^3, the mice were divided into three groups (6 mice per group) randomly. Indicated doses of SKLB826 and vehicle were administered once daily by intraperitoneal injection or oral dosing. Tumor volumes and body weight were measured every three days and clinical

symptoms were observed every day. The tumor volumes were calculated according to the following formula: Tumor volume (mm^3) = $0.52 \times L \times W^2$ (L represents length and W represents width).

Analysis of HepG2 tumor sections by immunohistochemistry and TUNEL assays

At the end of the animal experiments, tumors of HepG2 were collected, fixed and routinely processed and embedded in paraffin for immunohistochemical analysis and terminal deoxynucleotidyl transferase-mediated dUTP nick end-labeling (TUNEL) assay.

Sub-acute toxicity test

A sub-toxicity test was performed in healthy BALB/c mice which were orally administrated with a single dose of 2g/kg of SKLB826. The clinical symptoms of the mice, including mortality and body weights, were observed for 12 days. Then blood of the mice was obtained for serum biochemistry and hematological analysis using a Hitachi 7200 Blood Chemistry Analyzer and a Nihon Kohdern MEK-5216K Automatic Hematology Analyzer. The heart, liver, spleen, lung and kidney were fixed and routinely processed and embedded in paraffin for hematoxylin and eosin (H&E) staining analysis.

Statistical analysis

Statistical analyses were carried out in Microsoft Excel and GraphPad Prism. All data were expressed as mean ± standard deviation (SD) and statistically compared by one-way analysis of variance (ANOVA) followed by student's t-test. A statistically significant difference was defined as a p value less than 0.05.

Results

The inhibition effects of SKLB826 on proliferation of cancer cells

We used a panel of human cancer lines of different histotypes to investigate the anti-proliferating effects of SKLB826. The results showed that SKLB826 inhibited the proliferation of cancer cell with varying degrees (Fig. 2A). Interestingly human HCC cell lines were more sensitive to the treatment of SKLB826. So we chose HCC cell lines HepG2 and Bel7402 to further study the antitumor effects of SKLB826 and the

underlying mechanism. After treatment with SKLB826 for 24 h, 48 h and 72 h, respectively, the proliferation of both HepG2 and Bel7402 cell lines were decreased obviously with an IC_{50} values lessened from 10.6 μM to 2.05 μM for HepG2 and from 10.73 μM to 3.24 μM for Bel7402 (Fig. 2B). Moreover, we examined the inhibitory effects of SKLB826 on three normal cells (LO2, Vero and HEK293), while all the IC_{50} values were more than 40 μM (table 1). These data indicated that SKLB826 could inhibit the proliferation of hepatocellular carcinoma cells in a concentration- and time-dependent manner and no apparent toxicities were observed in normal cells.

The inhibition effects of SKLB826 on clonogenicity

Colony formation assays were performed to further validate the anti-proliferating effects of SKLB826. Notably, the colonies in treatment group became fewer and smaller than those in vehicle group (Fig. 2C), and when the concentration reached to 10 μM, almost no colony formation was observed in Bel7402 cell lines.

SKLB826 induced G2/M phase arrest of HCC cells

To further elucidate the molecular mechanism by which SKLB826 might suppress proliferation of HepG2 and Bel7402 cells, we examined the possible effects of SKLB826 on cell cycle distribution using FCM. As shown in Fig.3A, after exposure to SKLB826 for 24 h, the number of Bel7402 cells in G2/M phase increased significantly from 15.4% in the vehicle group to 19.5%, 24.7%, 39.2% and 51.5% in the groups treated with increasing concentrations of SKLB826. Similar results were observed in HepG2 cells (Fig. 3A). Meanwhile, an apparent reduction in G0/G1 phase was observed in HepG2 cell. From those data, we concluded that treatment with SKLB826 might inhibit proliferation of HCC through inducing G2/M phase arrest.

To get insight into the molecular mechanism underlying the cell cycle arrest, some cell cycle-related proteins were detected by western blotting, including some cyclin-dependent kinases (CDKs) and the cyclins. As shown in Fig. 3B, the level of CDK1 which could regulate the G2/M phase *via* combining with cyclin B to form the CDK1-cyclin B complex and with cyclinA2 which also regulated the G2/M phase decreased when the concentration of SKLB826 increased. The expression of cdc25c, which negatively regulate the CDK1-cyclin B complex [18], also decreased after treatment.

The above data indicated that SKLB826 induced the G2/M phase arrest *via* inhibiting the expression of CDK1,cdc25c and cyclinA2.

SKLB826 induced apoptosis of tumor cells

When investigating the cell cycle distribution, we observed that treatment with SKLB826 induced apoptosis of cancer cells. Therefore, Annexin V /PI staining was performed to further determine whether SKLB826 had a pro-apoptotic effect on HCC cell lines. As shown in Fig. 4A, after exposure of HepG2 cells to SKLB826 for 48 h, both the early apoptotic cells (Q3) and the late apoptotic cells (Q4) remarkably increased from 7.8% to 41.3% when the concentration increased from 5 to 20 μM, whereas nearly no cells undergoing apoptosis were detected in the vehicle group. Similar results were observed in the Bel7402 cells. Those data clearly indicated that SKLB826 induced the apoptosis of HepG2 and Bel7402 cells in a concentration-dependent manner. Furthermore, Hoechst 33342 staining was performed to exam the changes of cell morphology induced by SKLB826, HepG2 and Bel7402 cells were treated with SKLB826 for 24 h and the results displayed an evident appearance change. As shown in Fig. 4B, cell shrinkage and chromatin condensation (brighter-blue fluorescent) were observed in the HepG2 and Bel7402 cells. Arrowheads indicate cells exhibiting chromatin condensation, indicating the induction of apoptosis. Moreover, Western blotting also confirm the apoptosis, an increase in the levels of cleaved caspase 3 which is the main executor of apoptosis was observed after SKLB826 treatment for 48 hours in both cell lines (Fig. 4C).

As most types of chemotherapeutic drugs induced apoptosis via intrinsic pathway [12], we next investigated whether SKLB826 induced apoptosis in this way. Then western blotting was performed to detect the protein levels change of caspase family and Bcl-2 family proteins which were related to apoptosis. As shown in Fig. 4C, the results displayed that the levels of BAX increased while the levels of Bcl-2 decreased in both cell lines. We also detected the expression of cleaved caspase 9 which is involved in the mitochondria-mediated intrinsic apoptosis pathway [19]. As shown in Fig. 5A, the expression of cleaved caspase 9 increased visibly in a dose-dependent manner after treatment with SKLB826 for 48 h in both cell lines.

Effects of SKLB826 on the intrinsic apoptosis pathway

In the previous data, activation of cleaved caspase 9 was observed after treatment with SKLB826, and we also observed the increased level of BAX and the decreased level of Bcl-2 (Fig. 4C and 5A). We speculated that the apoptosis might be initiated through the mitochondria-mediated intrinsic pathway. Therefore, ROS levels of HepG2 and Bel7402 , which are generated in the mitochondria-mediated intrinsic pathway and significantly influenced the effect of various anticancer drugs on cancer cells [17], were detected using the fluorescent probe DCFH-DA after SKLB826 treatment. As shown in the Fig. 5B, ROS levels in HepG2 and Bel7402 elevated significantly, after cells were treated with escalating doses of SKLB826.

Mitochondria-mediated intrinsic apoptotic pathway is always accompanied by the disruption of mitochondrial membrane potential ($\Delta\Psi$m). We further investigated the alterations of mitochondrial membrane potential in both cell lines after treatment with SKLB826 by flow cytometry using green fluorochrome rhodamine 123 (Rh123). The results in Fig. 5C showed that $\Delta\Psi$m decreased after treatment with increasing concentrations of SKLB826, indicating the collapse of the mitochondrial potential induced by SKLB826. The data above suggested that SKLB826 induced apoptosis probably through intrinsic mitochondrial apoptotic pathway.

SKLB826 inhibited HepG2 xenograft growth in nude mice

To explore the anti-HCC effects of SKLB826 *in vivo*, HepG2 tumor bearing BALB/c nude mice models were established and treated with SKLB826 at doses of 100 (i.p) and 150 mg (p.o)/kg/day, respectively. As shown in Fig. 6A, the tumor was inhibited after treatment with SKLB826 compared with the vehicle treated group, and the inhibition rates of tumor volumes are 63.12% (i.p) and 51.63% (p.o). Furthermore, SKLB826 treatment was well tolerated and did not cause significant body weight loss (Fig. 6B).

To further investigate the mechanism of the anti-tumor effects of SKLB826 *in vivo*, immunohistochemical analysis and TUNEL staining were performed on tumor tissues from HepG2 models. As shown in Fig. 6C and 6D, the number of proliferating cells which was Ki67-positive in tumor tissues decreased and the TUNEL-positive cells in

SKLB826-treated group increased compared with the vehicle group. The data demonstrated that SKLB826 could suppress tumor growth *in vivo* through inhibiting proliferation and inducing apoptosis.

Safety profile of SKLB826

To determine the potential toxicity of SKLB826, a sub-acute test was performed in BALB/c mice. As shown in Fig.7A and B, after a single administration of SKLB826 at 2g/kg, no significant changes were observed in hematological and serum biochemical values and body weights compared with the vehicle group after 2 weeks. Moreover, microscopic examination in the heart, liver, spleen, lung and kidneys further displayed that SKLB826 treatment did not cause significant toxicity on mice.

Discussion

Nowadays, incidence and mortality of HCC have risen to the second place of cancer-related mortality in the world [21], but current therapies haven't been effective. Given that benzothiazole derivatives were regarded as a new and ideal sources for anti-HCC drug [22,23], a series of novel benzothiazole derivatives with good activities were designed and synthesized in our group, in which an optimized compound SKLB826 was obtained. In this report, we investigated the effects of SKLB826 on inhibiting HCC and the possible mechanism. Through the MTT assay, we found that SKLB826 displayed strong anti-proliferating activities against a broad spectrum of human cancer cell lines. Among those cells, HepG2 and Bel7402 were most sensitive to its treatment with IC_{50} values of 4.01 and 5.42 μM after 48 hours treatment, respectively. We further studied the inhibitory activity using colony formation assay. Moreover, SKLB826 had no apparent toxicity (Table 1) on the viabilities of normal cells. All the above data indicated that SKLB826 might be a promising anti-HCC drug with good efficacy and low toxicity. Next we investigated the possible mechanism of the proliferating inhibitory effects, and the results revealed that SKLB826 could induce remarkable G2/M phase arrest and apoptosis in the two hepatocarcinoma cell lines.

The endogenous regulation of cell cycle is mainly controlled by cell cycle checkpoints which help to confirm the accuracy of DNA replication and division. Cell cycle checkpoints are regulated by a family of cyclin-dependent kinases (CDKs) which are regulated *via* combining with a various of protein, especially, the cyclins [4, 24]. In the G2 phase, CDK1 (cdc2), which is an important regulator that controls cells from G2 phase into M phase, forms a complex with cyclinB1 and regulates the mitosis by its phosphorylation state. CyclinB1-CDK1 complex is activated after dephosphorylation of CDK1 at Thr14 and Tyr15 by the protein phosphatase cdc25c [25], then the activating cyclinB1-CDK1 complex moved into the nucleus and the mitosis starts. Therefore, CDK1 and cdc25c play important roles in G2/M phase regulation [26,27]. In our study, we found that SKLB826 remarkably induced G2/M arrest in HepG2 and Bel7402 cell lines, so we chose to investigate the change of G2/M related proteins and we found SKLB826 treatment significantly decreased the expression of cdc25c and CDK1. Furthermore, some studies have been reported recently that cyclinA2 can combine with CDK1 and the cyclinA2-CDK1 complex can activate the cyclinB1-CDK1 complex in proliferating somatic cells [28]. To further investigate the mechanism of the G2/M phase arrest induced by SKLB826, the expression of cyclinA2 was measured. In our study, we found that the levels of cyclinA2 down regulated, which further validated that SKLB826 treatment caused G2/M arrest.

Defects in the G2/M arrest may disrupt the ability of a damaged cell to enter mitosis and finally undergo apoptosis [29]. There are two kinds of apoptotic pathways, extrinsic pathway and intrinsic pathway. In mitochondria-mediated intrinsic apoptosis pathway, upon receiving a death signal, the permeability of outer mitochondrial membrane increases and $\Delta\Psi m$ decreases, then cytochrome c is released which can bind to apoptotic protease-activating factor 1 (Apaf-1). It leads to cleavage of caspase-9, which then induce activation of downstream caspase-3 and caspase-7 to trigger apoptosis [30]. Likewise, Bcl-2 family proteins are associated with this intrinsic apoptosis [31]. In our study, after treatment of HepG2 and Bel7402 cell with SKLB826, the levels of pro-apoptotic protein BAX in HepG2 and Bel7402 cells were upregulated while the levels of anti-apoptotic protein Bcl-2 were downregulated. In addition, increase of

cleaved caspase3, 9 expression and decrease of $\Delta\Psi m$ were also observed, indicating that the intrinsic apoptotic pathway was probably activated after treatment with SKLB826.

A various of studies have proven that increase of ROS is associated with the intrinsic apoptosis and G2/M phase cell cycle arrest induced by anticancer agents [32,33]. In this study, the level of ROS in HCC was increased in a dose-dependent manner after treatment with SKLB826, suggesting that SKLB816 induced apoptosis mainly through the intrinsic apoptotic pathway.

Not all small-molecule compounds exhibiting antitumor activity *in vitro* display anticancer activity *in vivo*, we therefore further studied the activity of SKLB826 *in vivo* using HepG2 tumor model established in nude mice. The results in our study showed that SKLB826 inhibited the growth of tumor with an inhibitory rate of 63.12% at the doses of 100 mg/kg (i.p) with no apparent toxicity was observed. Moreover, the results of immunohistochemistry and TUNEL staining revealed SKLB826 could decrease proliferation and induce apoptosis of tumor cells in tumor sections, as shown by decreased Ki67-positive cells and increased green fluorescence signal in TUNEL assay.

Although SKLB826 had a good effect of anti-tumor and solubility, there still were some weaknesses, for example, pharmacokinetic properties of SKLB826 were poor, which might affect the effects of SKLB826 on anti-tumor (data were not shown). Therefore, we will continue to optimize the structure of SKLB826 to improve the pharmacokinetic properties.

In conclusion, through constantly optimizing the structure of benzothiazole derivatives, we got the compound SKLB826 which had remarkable efficacy to inhibit human liver cancer *in vitro* and *in vivo*. *In vitro*, SKLB826 inhibited cell cycle progression *via* inhibiting the activities of the cyclinA2 and cyclinB1-CDK1 complex and further induced apoptosis through the mitochondria-mediated intrinsic pathway. *In vivo*, SKLB826 displayed a strong antitumor activity in the human liver cancer xenograft without causing any significant toxicities. In addition, the synthesis of SKLB826 is easy to achieve. Hence, the compelling evidence indicated that SKLB826 may be a potential candidate for the development of new anti-HCC drug.

Reference

1   K. J. Lafaro, A. N. Demirjian and T. M. Pawlik, *Surgical oncology clinics of North America* **2015**, *24*, 1-17;

2   W.-Y. Lau and E. C. H. Lai, *Hepatobiliary & Pancreatic Diseases International* **2008**, *7*, 237-257.

3   L. Rossi, F. Zoratto, A. Papa, F. Iodice, M. Minozzi, L. Frati and S. Tomao, *World J Gastrointest Oncol* **2010**, *2*, 348-359.

4   R. S. DiPaola, *Clinical cancer research* **2002**, *8*, 3311-3314.

5   G. K. Schwartz and M. A. Shah, *Journal of clinical oncology* **2005**, *23*, 9408-9421;

6   S. Diaz-Moralli, M. Tarrado-Castellarnau, A. Miranda and M. Cascante, *Pharmacology & therapeutics* **2013**, *138*, 255-271.

7   K. L. Barton, M. Gromeier, K. Misuraca, D. G. Kirsch, F. Cordero, O. J. Becher and E. Dobrikova, *PLOS ONE* **2013**, *8*, 1-7.

8   K. Samson, *Oncology Times* **2014**, *36*, 39-40.

9   Y. Liao, H. Bai, Z. Li, J. Zou, J. Chen, F. Zheng, J. Zhang, S. Mai, M. Zeng and H. Sun, *Cell death & disease* **2014**, *5*, e1137.

10   S. W. Fesik, *Nature Reviews Cancer* **2005**, *5*, 876-885;

11   Y. Zhu, Y. Xia, T. Ye, X. Shi, X. Song, L. Liu, J. Zeng, N. Wang, Y. Luo and Y. Han, *Cellular Physiology and Biochemistry* **2014**, *33*, 933-944.

12   M. S. Soengas and S. W. Lowe, *Oncogene* **2003**, *22*, 3138-3151.

13   I. M. Ghobrial, T. E. Witzig and A. A. Adjei, *A Cancer Journal for Clinicians* **2005**, *55*, 178-194.

14   S. H. L. Kok, R. Gambari, C. H. Chui, M. C. W. Yuen, E. Lin, R. S. M. Wong, F. Y. Lau, G. Y. M. Cheng, W. S. Lam and S. H. Chan, *Bioorganic & medicinal chemistry* **2008**, *16*, 3626-3631.

15   X.-H. Shi, Z. Wang, Y. Xia, T.-H. Ye, M. Deng, Y.-Z. Xu, Y.-Q. Wei and L.-T. Yu, *Molecules* **2012**, *17*, 3933-3944.

16   Y. Xia, X. Song, D. Li, T. Ye, Y. Xu, H. Lin, N. Meng, G. Li, S. Deng and S. Zhang, *Scientific reports* **2014**, *4*, 1-10.

17   R. C. Scaduto, Jr. and L. W. Grotyohann, *Biophys J* **1999**, *76*, 469-477.

18   C. G. Takizawa and D. O. Morgan, *Current opinion in cell biology* **2000**, *12*, 658-665.

19   S. Fulda and K. Debatin, *Oncogene* **2006**, *25*, 4798-4811.

20   Y. Xia, Q. Lei, Y. Zhu, T. Ye, N. Wang, G. Li, X. Shi, Y. Liu, B. Shao and T. Yin, *Cancer letters* **2014**, *355*, 297-309.

21   Z.-F. Li, *World Journal of Gastroenterology* **2009**, *15*, 4538.

22   A. Villanueva and J. M. Llovet, *Gastroenterology* **2011**, *140*, 1410-1426.

23   Z. Wang, X.-H. Shi, J. Wang, T. Zhou, Y.-Z. Xu, T.-T. Huang, Y.-F. Li, Y.-L. Zhao, L. Yang and S.-Y. Yang, *Bioorganic & medicinal chemistry letters* **2011**, *21*, 1097-1101.

24   M. Malumbres and M. Barbacid, *Nature Reviews Cancer* **2009**, *9*, 153-166.

25   O. Gavet and J. Pines, *Developmental cell* **2010**, *18*, 533-543.

26   L. Fletcher, Y. Cheng and R. J. Muschel, *Cancer research* **2002**, *62*, 241-250;

27   M. Jackman, C. Lindon, E. A. Nigg and J. Pines, *Nature cell biology* **2003**, *5*, 143-148.

28   C. Badie, J. Bourhis, J. Sobczak-Thepot, H. Haddada, M. Chiron, M. Janicot, F. Janot, T. Tursz and G. Vassal, *British journal of cancer* **2000**, *82*, 642-650.

29   Y.-C. Hseu, M.-S. Lee, C.-R. Wu, H.-J. Cho, K.-Y. Lin, G.-H. Lai, S.-Y. Wang, Y.-H. Kuo, K. Senthil Kumar and H.-L. Yang, *Journal of agricultural and food chemistry* **2012**, *60*, 2385-2397.

30   K. M. Boatright and G. S. Salvesen, *Current opinion in cell biology* **2003**, *15*, 725-731.

31   M. H. Kang and C. P. Reynolds, *Clinical cancer research* **2009**, *15*, 1126-1132.

32   H.-U. Simon, A. Haj-Yehia and F. Levi-Schaffer, *Apoptosis* **2000**, *5*, 415-418;

33   D. Xiao, A. Herman-Antosiewicz, J. Antosiewicz, H. Xiao, M. Brisson, J. S. Lazo and S. V. Singh, *Oncogene* **2005**, *24*, 6256-6268.

Tables and illustrations
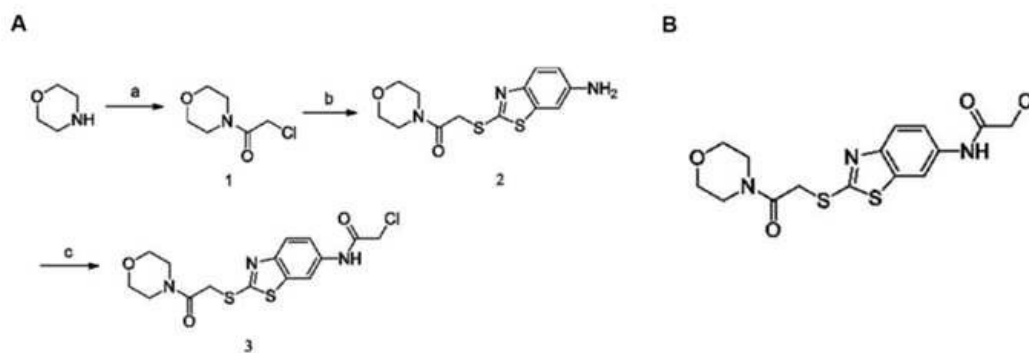
Fig.1 The synthetic route and structure of SKLB826. (A) The starting material 1 was prepared from morpholine and 2-chloroacetyl chloride at room temperature. Treatment of 6-aminobenzo[*d*]thiazole-2-thiol with 1 in THF provided 2 following by 2-chloroacetyl chloride treatment of a mixture of 2 and K_2CO_3. Then, SKLB826 was obtained. Reagents and conditions: (a) 2-chloroacetyl chloride, CH_2Cl_2, NEt_3, rt, 4 h; (b) 6-aminobenzo[*d*]thiazole-2-thiol, THF, K_2CO_3, reflux, 5 h; (c) 2-chloroacetyl chloride, CH_2Cl_2, K_2CO_3, rt, 4 h. (B) The chemical structure of SKLB826.
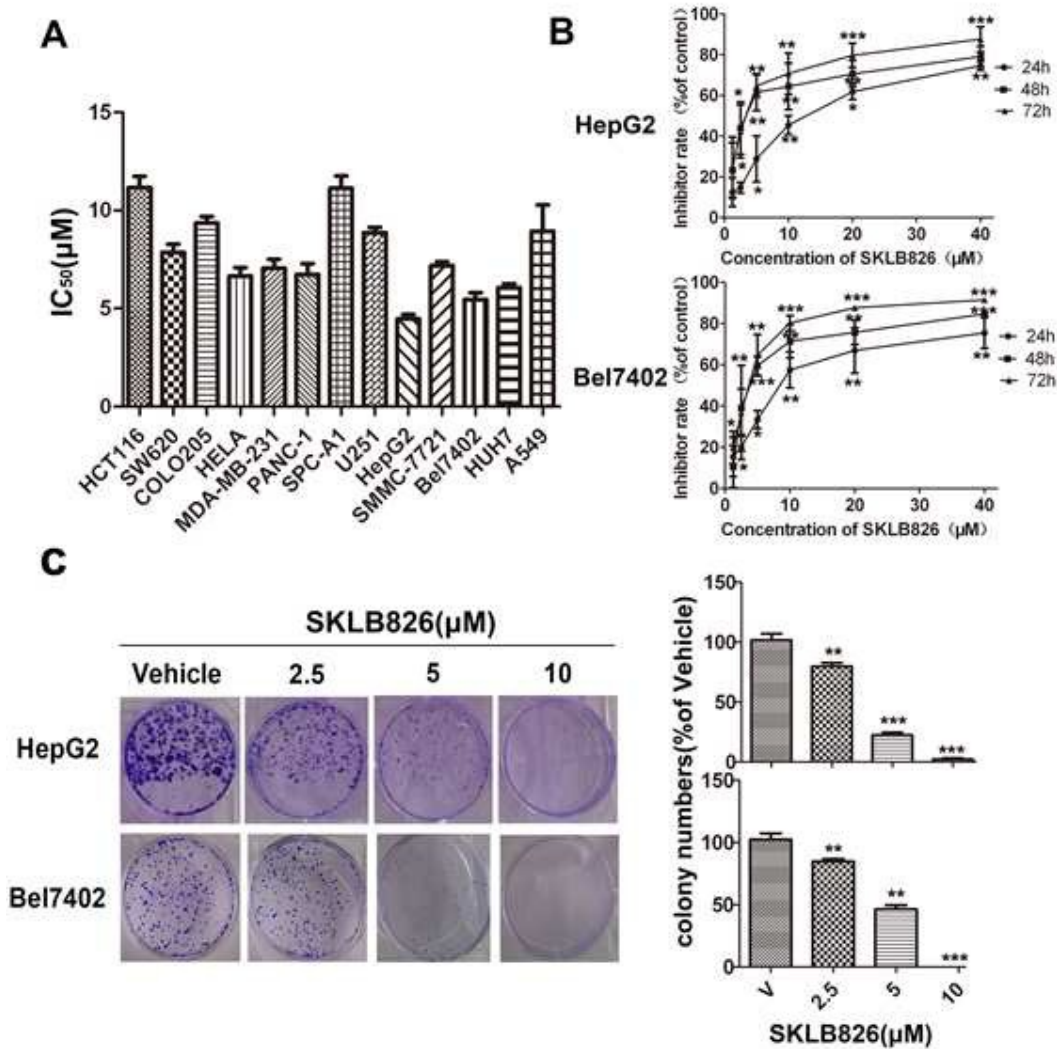
Figure 2. Inhibition of cell growth and colony formation in human cancer cell lines by SKLB826. (A) The proliferation inhibitory effects of SKLB826 on human cancer cells. IC_{50} values were expressed as mean$\pm$SD for 3 independent experiments. (B) HepG2 and Bel7402 cell lines were treated with increasing doses of SKLB826 for 24 h, 48 h and 72 h, respectively. Each point represents the mean$\pm$ SD for 3 independent experiments (*$p<0.05$, **$p<0.01$, ***$p<0.001$ vs vehicle control). (C) Effects of SKLB826 on cell colony formation after treated for two weeks. Quantification is shown in the right panel. Data are expressed as mean$\pm$SD for 3 independent experiments (*$p<0.05$, **$p<0.01$, ***$p<0.001$ vehicle control).

Table 1. The effects of SKLB826 on normal cell lines viability. Each cell line was treated with SKLB826 for 48 h and MTT assay was used to determined the IC_{50} values. Data are expressed   as mean$\pm$SD for 3 independent experiments.

Cell lines	Cell type	$IC_{50}(\mu M)$
HEK293	Human embryonic kidney cell line	>40
LO2	Human normal liver cell line	>40
Vero	African monkey kidney cell line	>40
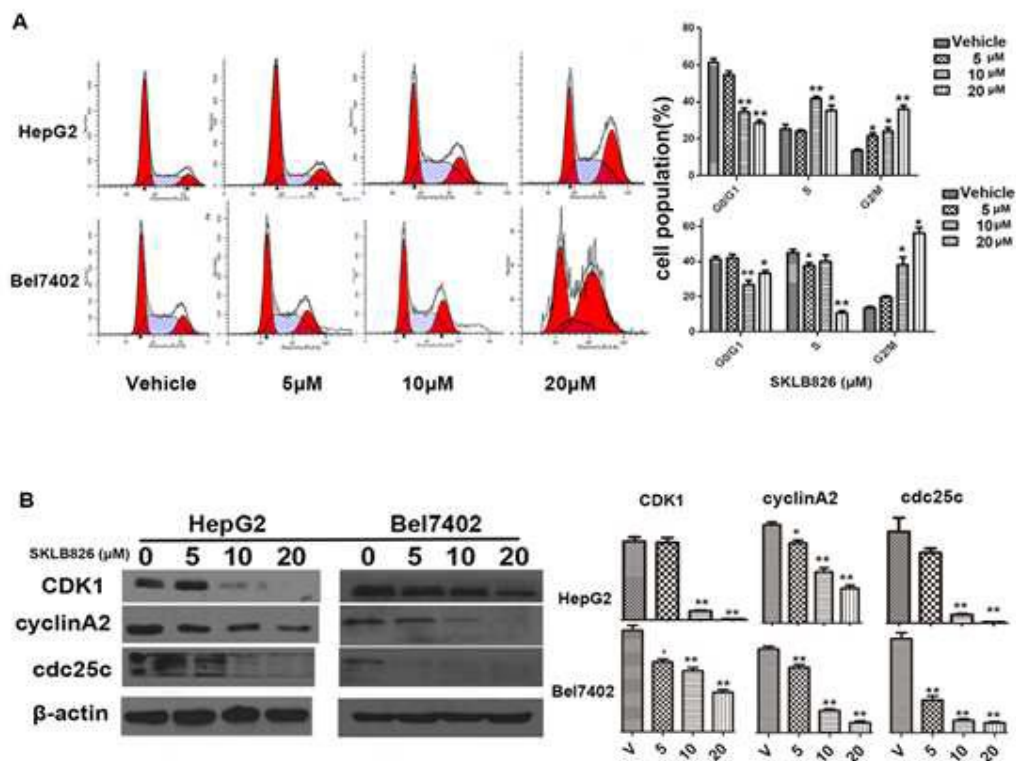
Figure 3. SKLB826 inhibited the proliferation and induced G2/M phase arrest of HCC cells. (A) HepG2 and Bel7402 cells were treated with escalating doses of SKLB826 (0, 5, 10 and 20 μM) for 24 h and stained with 50 μg/mL propidium iodide (PI). Then the stained cells were assayed by flow cytometry. Quantification of cell cycle distribution is shown in the right panel. Data are expressed as mean ±SD for 3 independent experiments. (B) Effects of SKLB826 on expression of G2/M phase related regulator proteins. The expressions of CDK1, cyclinA2 and cdc25c decreased after treatment with SKLB826 for 48 h at indicated concentrations (0, 5, 10 and 20 μM). Protein expression was qualified by the densitometry analysis using Image J (shown in the right panel).Columns, mean; bars, SD, (*p<0.05, **p<0.01, ***p<0.001 vehicle control).
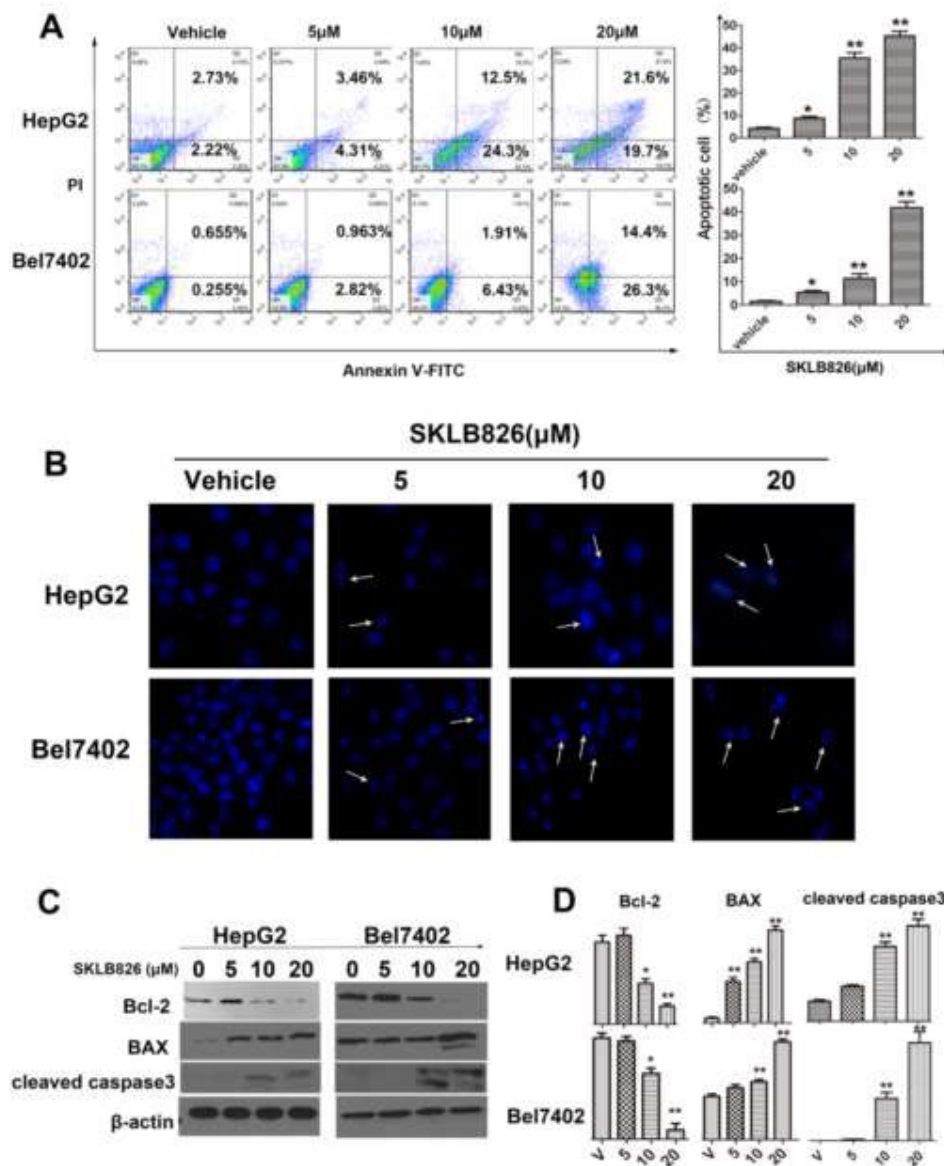
Figure 4. SKLB826 induced apoptosis of HepG2 and Bel7402 cell lines. (A) HepG2 and Bel7402 cells were treated with SKLB826 for 24 h and apoptosis was detected by flow cytometry after Annexin V/PI staining. (B) Cell morphological alterations and nuclear changes of HepG2 and Bel7402 cells were determined by staining with Hoechst33342 (10 μg/mL) and visualized by microscope after treatment with increasing doses of SKLB826 for 24 h. (C) The levels of Bcl-2, BAX and cleaved caspase 3 were determined *via* western blotting. Protein expressions were qualified by the densitometry analysis using Image J (shown in the right panel). Data are expressed as mean $\pm$ SD for 3 independent experiments. Columns, mean; bars, SD, (*p<0.05, **p<0.01, ***p<0.001).
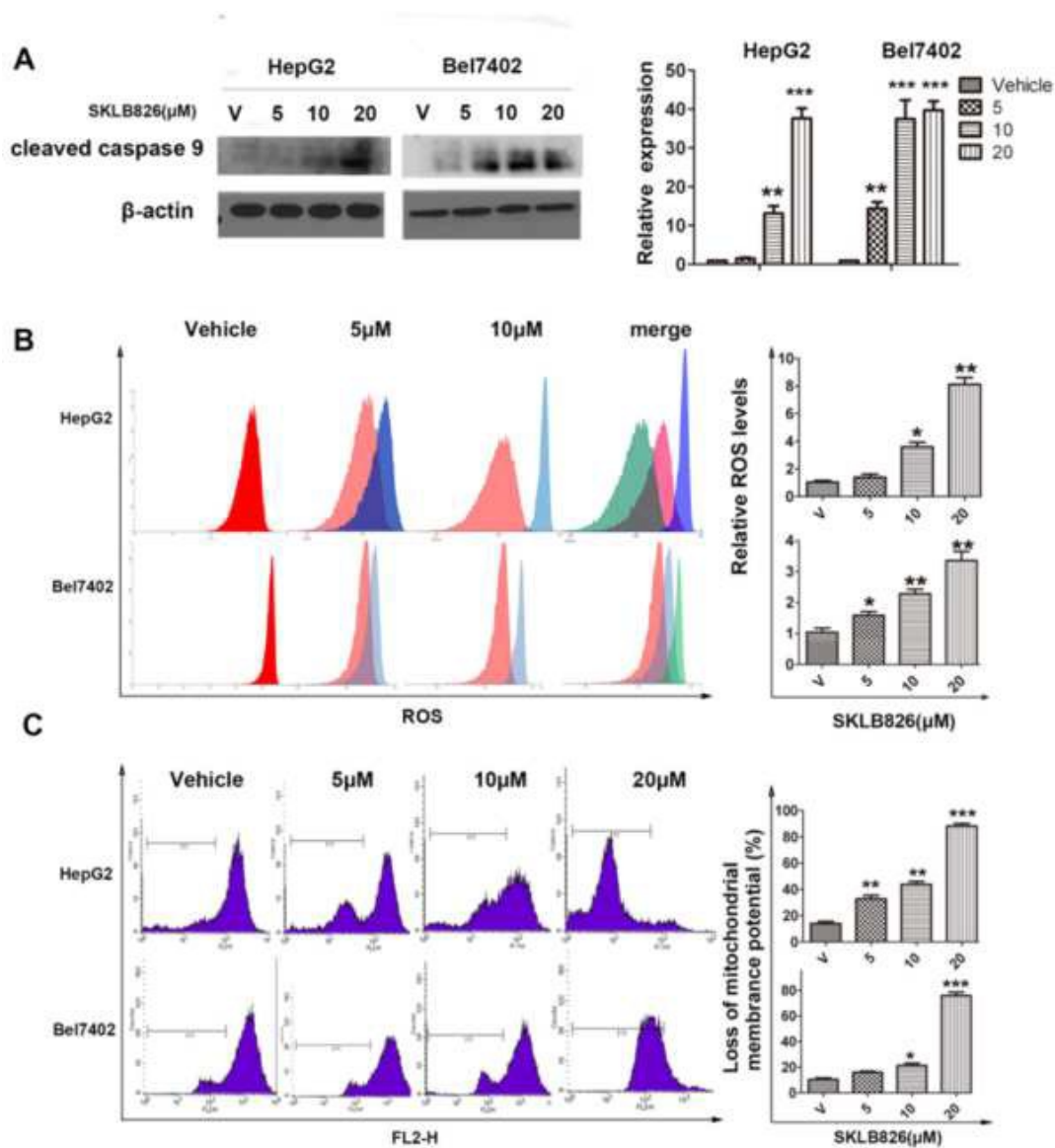
Figure 5. Effects of SKLB826 on the intrinsic apoptosis pathway. (A)The expression of typical intrinsic apoptosis-related protein was determined by western blot. HepG2 and Bel7402 cells were treated with SKLB826 for 48h, then the expression of cleaved caspase 9 was detected via western blot. Protein expressions were qualified by the densitometry analysis using Image J (shown in the right panel). Data are expressed as mean±SD for 3 independent experiments. (B) HepG2 and Bel7402 were treated with SKLB826 for 12h, and then ROS levels in cells were measured by FCM. Data are expressed as mean±SD for 3 independent experiments. (C) Changes of the mitochondrial membrane potential of HepG2 and Bel7402 cells were detected by FCM after treatment with SKLB826 for 24 h. Data are expressed as mean±SD for 3 independent experiments. Quantification is shown in the right panel. Columns, mean; bars, SD. (*p<0.05, **p<0.01, ***p<0.001).
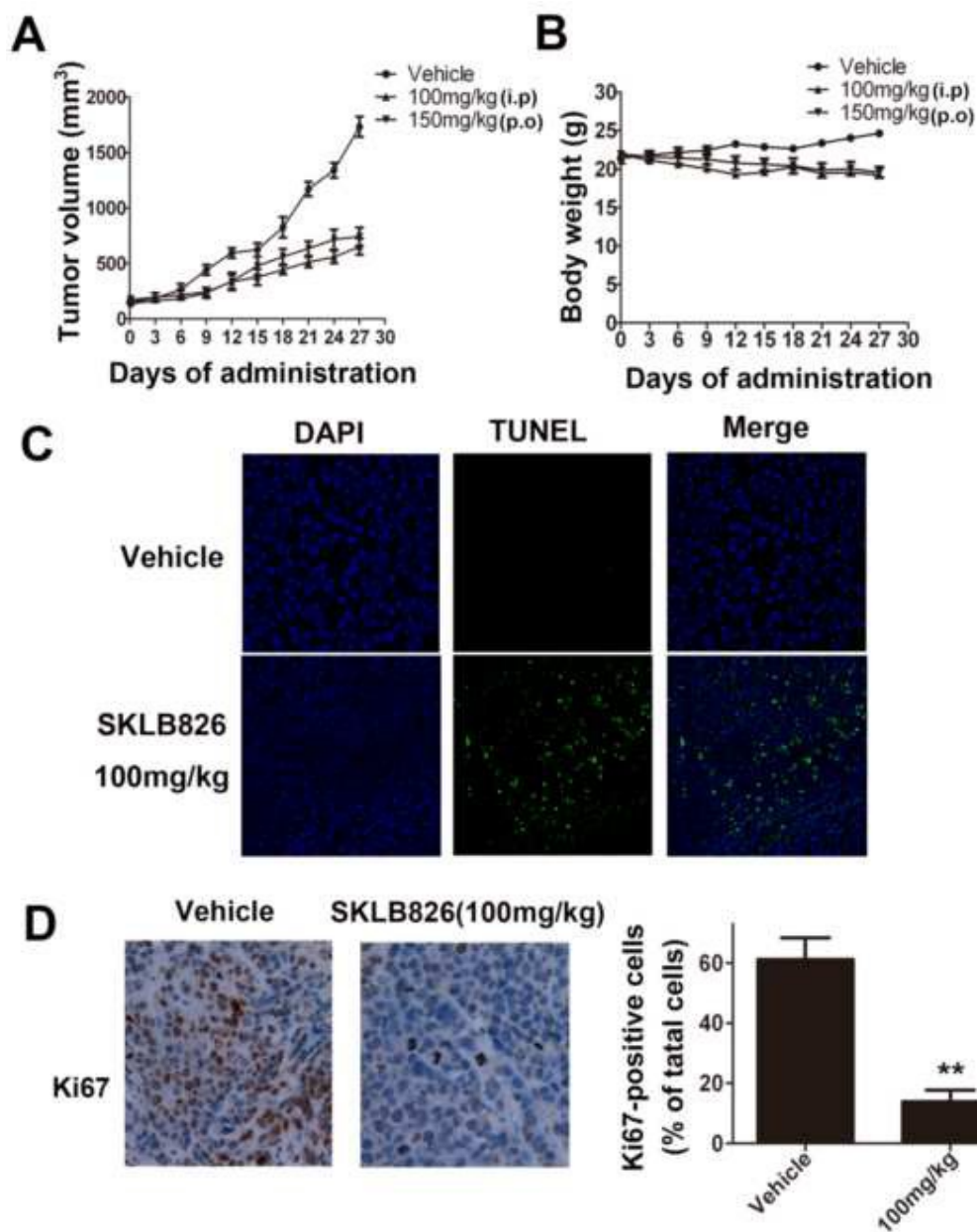
Figure 6. Effect of SKLB826 on HepG2 tumor xenograft growth in *vivo*. (A and B) HepG2 cells were subcutaneously inoculated into the nude mice. Then animals were treated with 100 mg/kg (i.p), 150 mg/kg (p.o) of SKLB826 or vehicle everyday. Tumor volumes and body weights were measured every three days. Data are expressed as mean$\pm$SD (n=5). (C) After treatment with SKLB826 for 4 weeks, apoptotic cells in tumor tissues were measured by TUNEL assay. (D) The Ki67 expression in tumor xenograft tissues was determined via using immunohistochemistry and the Ki67-positive cells were counted in five high power fields, data were summarized in terms of percent positive cells (right panel). Columns, mean; bars, SD. (*$p<0.05$, **$p<0.01$, ***$p<0.001$).
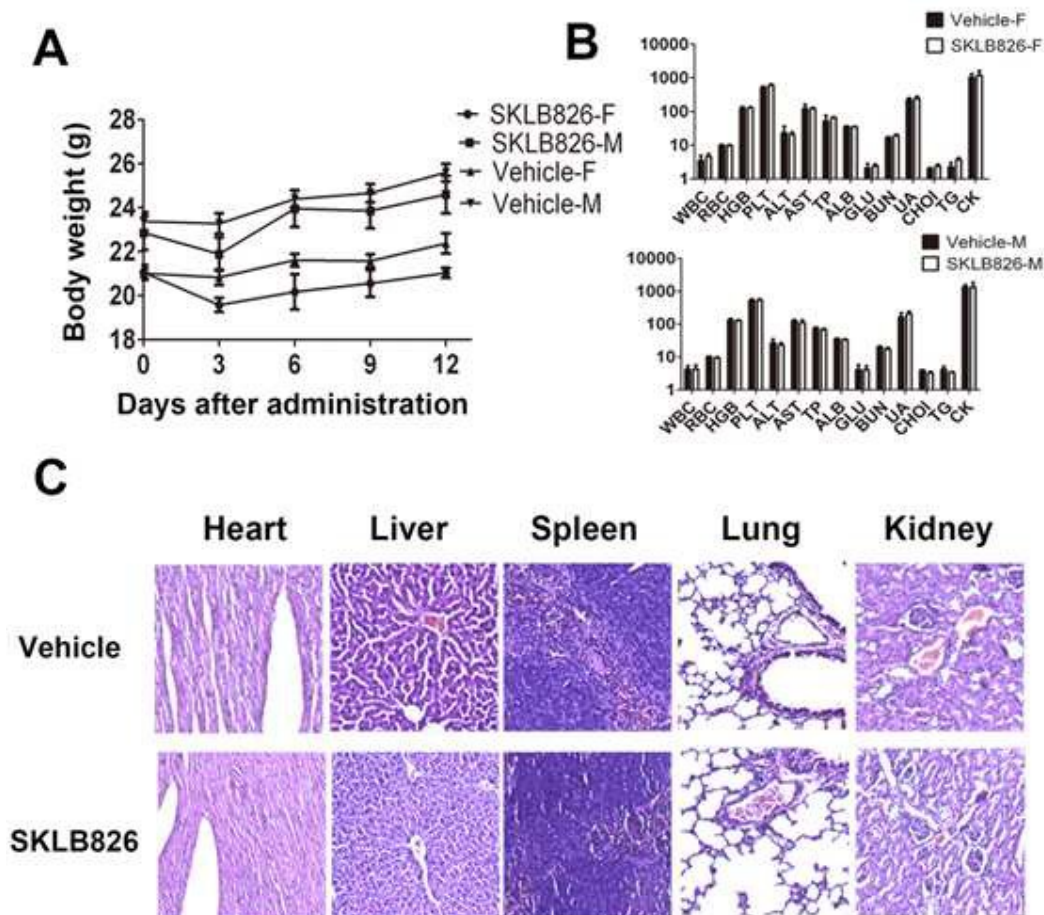
Figure 7. Preliminary safety evaluation of SKLB826 in BALB/c mice. Mice were divided into 4 groups and intraperitoneally administrated with a single dose of SKLB826 (2g/kg). After two weeks, animals were sacrificed and the main organs and blood were obtained for further study. (A) The difference of body weights between two administrated group (female and male mice) and two vehicle groups (female and male mice) were not significant. Data are expressed as mean±SD (n=5). (B) The parameters of blood routine and blood biochemical analysis were determined. There is no significant difference between SKLB826 administrated group (female and male mice) and two vehicle control group (female and male mice). Data are expressed as mean±SD (n=5), Columns, mean; bars, SD. (C) Pathologic change in tissues was observed after treatment with SKLB826 which did not cause obviously different. The units of the parameters are as follows. WBC (white blood cell) and PLT (platelet),10^9/L; RBC (red blood cell), 10^{12}/L; HGB (hemoglobin), ALB (albumin) and TP (total protein), g/L; ALT (alanine transarninase), AST (aspartate aminotransferase) and CK (cre-atinine kinase), U/L; UA (uric acid); GHO (cholesterol), BUN (blood urea nitrogen), GLU (glucose) and TG (triglyceride), mM. Organs (heart, liver, spleen, lung, kidney) were fixed in 4% paraformaldehyde, processed for paraffin embedding and then stained by hematoxylin and eosin (×20). Images shown are representatives from each group.